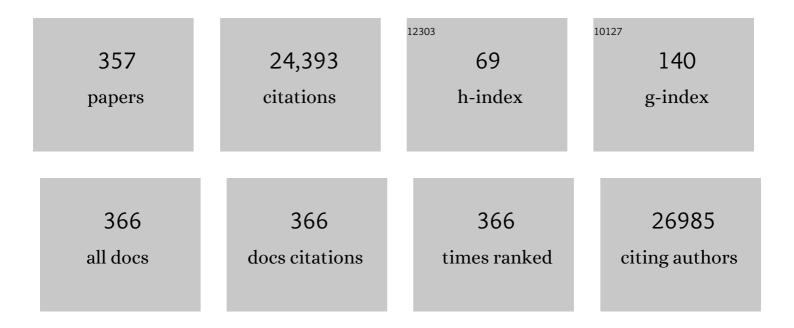
List of Publications by Year in descending order

Source: https://exaly.com/author-pdf/8605052/publications.pdf

Version: 2024-02-01



#	Article	IF	CITATIONS
1	Doping Metal–Organic Frameworks for Water Oxidation, Carbon Dioxide Reduction, and Organic Photocatalysis. Journal of the American Chemical Society, 2011, 133, 13445-13454.	6.6	1,363
2	Postsynthetic Modifications of Iron-Carboxylate Nanoscale Metalâ^'Organic Frameworks for Imaging and Drug Delivery. Journal of the American Chemical Society, 2009, 131, 14261-14263.	6.6	1,354
3	Highly luminescent S, N co-doped graphene quantum dots with broad visible absorption bands for visible light photocatalysts. Nanoscale, 2013, 5, 12272.	2.8	1,018
4	Electrospinning of polymeric nanofibers for drug delivery applications. Journal of Controlled Release, 2014, 185, 12-21.	4.8	995
5	Formation mechanism and optimization of highly luminescent N-doped graphene quantum dots. Scientific Reports, 2014, 4, 5294.	1.6	759
6	On–Off–On Fluorescent Carbon Dot Nanosensor for Recognition of Chromium(VI) and Ascorbic Acid Based on the Inner Filter Effect. ACS Applied Materials & Interfaces, 2013, 5, 13242-13247.	4.0	700
7	Porous Phosphorescent Coordination Polymers for Oxygen Sensing. Journal of the American Chemical Society, 2010, 132, 922-923.	6.6	587
8	Integrating Oxaliplatin with Highly Luminescent Carbon Dots: An Unprecedented Theranostic Agent for Personalized Medicine. Advanced Materials, 2014, 26, 3554-3560.	11.1	509
9	Fast Response and High Sensitivity Europium Metal Organic Framework Fluorescent Probe with Chelating Terpyridine Sites for Fe ³⁺ . ACS Applied Materials & Interfaces, 2013, 5, 1078-1083.	4.0	488
10	Self-Targeting Fluorescent Carbon Dots for Diagnosis of Brain Cancer Cells. ACS Nano, 2015, 9, 11455-11461.	7.3	439
11	Nanoscale metal–organic frameworks for drug delivery: a conventional platform with new promise. Journal of Materials Chemistry B, 2018, 6, 707-717.	2.9	413
12	Highly Stable and Porous Cross-Linked Polymers for Efficient Photocatalysis. Journal of the American Chemical Society, 2011, 133, 2056-2059.	6.6	394
13	Tailoring color emissions from N-doped graphene quantum dots for bioimaging applications. Light: Science and Applications, 2015, 4, e364-e364.	7.7	366
14	Stimuli-Responsive Polymersomes for Biomedical Applications. Biomacromolecules, 2017, 18, 649-673.	2.6	316
15	Light-Activatable Red Blood Cell Membrane-Camouflaged Dimeric Prodrug Nanoparticles for Synergistic Photodynamic/Chemotherapy. ACS Nano, 2018, 12, 1630-1641.	7.3	300
16	Three Colors Emission from S,N Coâ€doped Graphene Quantum Dots for Visible Light H ₂ Production and Bioimaging. Advanced Optical Materials, 2015, 3, 360-367.	3.6	276
17	H ₂ O ₂ -Responsive Vesicles Integrated with Transcutaneous Patches for Glucose-Mediated Insulin Delivery. ACS Nano, 2017, 11, 613-620.	7.3	255
18	One-Pot To Synthesize Multifunctional Carbon Dots for Near Infrared Fluorescence Imaging and Photothermal Cancer Therapy. ACS Applied Materials & Interfaces, 2016, 8, 23533-23541.	4.0	244

#	Article	IF	CITATIONS
19	lodinated Nanoscale Coordination Polymers as Potential Contrast Agents for Computed Tomography. Angewandte Chemie - International Edition, 2009, 48, 9901-9904.	7.2	229
20	Metal–Organic Framework@Porous Organic Polymer Nanocomposite for Photodynamic Therapy. Chemistry of Materials, 2017, 29, 2374-2381.	3.2	204
21	Freeze Drying Significantly Increases Permanent Porosity and Hydrogen Uptake in 4,4â€Connected Metal–Organic Frameworks. Angewandte Chemie - International Edition, 2009, 48, 9905-9908.	7.2	203
22	Nanoscale Polymer Metal–Organic Framework Hybrids for Effective Photothermal Therapy of Colon Cancers. Advanced Materials, 2016, 28, 9320-9325.	11.1	194
23	One-Step Synthesis of Nanoscale Zeolitic Imidazolate Frameworks with High Curcumin Loading for Treatment of Cervical Cancer. ACS Applied Materials & amp; Interfaces, 2015, 7, 22181-22187.	4.0	192
24	Second Near-Infrared Conjugated Polymer Nanoparticles for Photoacoustic Imaging and Photothermal Therapy. ACS Applied Materials & Interfaces, 2018, 10, 7919-7926.	4.0	188
25	BODIPY-containing nanoscale metal–organic frameworks for photodynamic therapy. Chemical Communications, 2016, 52, 5402-5405.	2.2	160
26	Enhanced activation of STAT pathways and overexpression of survivin confer resistance to FLT3 inhibitors and could be therapeutic targets in AML. Blood, 2009, 113, 4052-4062.	0.6	144
27	Identification of a Novel Family of Nonclassic Yeast Phosphatidylinositol Transfer Proteins Whose Function Modulates Phospholipase D Activity and Sec14p-independent Cell Growth. Molecular Biology of the Cell, 2000, 11, 1989-2005.	0.9	140
28	Pleiotropic Alterations in Lipid Metabolism in Yeast <i>sac1</i> Mutants: Relationship to "Bypass Sec14p― and Inositol Auxotrophy. Molecular Biology of the Cell, 1999, 10, 2235-2250.	0.9	138
29	Yeast Sec14p Deficient in Phosphatidylinositol Transfer Activity Is Functional In Vivo. Molecular Cell, 1999, 4, 187-197.	4.5	131
30	Controlled release of urea encapsulated by starch-g-poly(l-lactide). Carbohydrate Polymers, 2008, 72, 342-348.	5.1	128
31	Tailor-Made Semiconducting Polymers for Second Near-Infrared Photothermal Therapy of Orthotopic Liver Cancer. ACS Nano, 2019, 13, 7345-7354.	7.3	126
32	Porphyrinâ€Based Carbon Dots for Photodynamic Therapy of Hepatoma. Advanced Healthcare Materials, 2017, 6, 1600924.	3.9	125
33	Nanoscale Mixed-Component Metal–Organic Frameworks with Photosensitizer Spatial-Arrangement-Dependent Photochemistry for Multimodal-Imaging-Guided Photothermal Therapy. Chemistry of Materials, 2018, 30, 6867-6876.	3.2	122
34	Co-delivery of daunomycin and oxaliplatin by biodegradable polymers for safer and more efficacious combination therapy. Journal of Controlled Release, 2012, 163, 304-314.	4.8	110
35	A novel polymer–paclitaxel conjugate based on amphiphilic triblock copolymer. Journal of Controlled Release, 2007, 117, 210-216.	4.8	108
36	Engineering Metal–Organic Frameworks for Photoacoustic Imaging-Guided Chemo-/Photothermal Combinational Tumor Therapy. ACS Applied Materials & Interfaces, 2018, 10, 41035-41045.	4.0	104

#	Article	IF	CITATIONS
37	Direct Formation of Giant Vesicles from Synthetic Polypeptides. Langmuir, 2007, 23, 8308-8315.	1.6	103
38	Redox-Hypersensitive Organic Nanoparticles for Selective Treatment of Cancer Cells. Chemistry of Materials, 2016, 28, 4440-4446.	3.2	101
39	Paclitaxel dimers assembling nanomedicines for treatment of cervix carcinoma. Journal of Controlled Release, 2017, 254, 23-33.	4.8	101
40	Diketopyrrolopyrrole-based carbon dots for photodynamic therapy. Nanoscale, 2018, 10, 10991-10998.	2.8	101
41	Colour-tunable ultralong-lifetime room temperature phosphorescence with external heavy-atom effect in boron-doped carbon dots. Chemical Engineering Journal, 2021, 420, 127647.	6.6	101
42	lodo-BODIPY: a visible-light-driven, highly efficient and photostable metal-free organic photocatalyst. RSC Advances, 2013, 3, 13417.	1.7	99
43	Unadulterated BODIPY nanoparticles for biomedical applications. Coordination Chemistry Reviews, 2019, 390, 76-85.	9.5	99
44	Inhibition of orthotopic secondary hepatic carcinoma in mice by doxorubicin-loaded electrospun polylactide nanofibers. Journal of Materials Chemistry B, 2013, 1, 101-109.	2.9	97
45	Synergistic co-delivery of doxorubicin and paclitaxel by porous PLGA microspheres for pulmonary inhalation treatment. European Journal of Pharmaceutics and Biopharmaceutics, 2014, 88, 1086-1093.	2.0	97
46	Poly(l-lactide)/starch blends compatibilized with poly(l-lactide)-g-starch copolymer. Carbohydrate Polymers, 2006, 65, 75-80.	5.1	96
47	Nanoparticles of Chlorin Dimer with Enhanced Absorbance for Photoacoustic Imaging and Phototherapy. Advanced Functional Materials, 2018, 28, 1706507.	7.8	96
48	Carbon Dots Based Nanoscale Covalent Organic Frameworks for Photodynamic Therapy. Advanced Functional Materials, 2020, 30, 2004680.	7.8	95
49	A Paclitaxel Prodrug Activatable by Irradiation in a Hypoxic Microenvironment. Angewandte Chemie - International Edition, 2020, 59, 23198-23205.	7.2	94
50	A dual-responsive nanocapsule via disulfide-induced self-assembly for therapeutic agent delivery. Chemical Science, 2016, 7, 1846-1852.	3.7	92
51	The use of cisplatin-loaded mucoadhesive nanofibers for local chemotherapy of cervical cancers in mice. European Journal of Pharmaceutics and Biopharmaceutics, 2015, 93, 127-135.	2.0	91
52	Hypoxia-Triggered Nanoscale Metal–Organic Frameworks for Enhanced Anticancer Activity. ACS Applied Materials & Interfaces, 2018, 10, 24638-24647.	4.0	91
53	AIE Multinuclear Ir(III) Complexes for Biocompatible Organic Nanoparticles with Highly Enhanced Photodynamic Performance. Advanced Science, 2019, 6, 1802050.	5.6	87
54	Fluorescent Hydrogen-Bonded Organic Framework for Sensing of Aromatic Compounds. Crystal Growth and Design, 2015, 15, 542-545.	1.4	86

#	Article	IF	CITATIONS
55	Endogenous Hydrogen Sulfide-Triggered MOF-Based Nanoenzyme for Synergic Cancer Therapy. ACS Applied Materials & Interfaces, 2020, 12, 30213-30220.	4.0	85
56	Doxorubicin-Loaded Carborane-Conjugated Polymeric Nanoparticles as Delivery System for Combination Cancer Therapy. Biomacromolecules, 2015, 16, 3980-3988.	2.6	81
57	Mitochondria-Localized Fluorescent BODIPY-Platinum Conjugate. ACS Medicinal Chemistry Letters, 2015, 6, 430-433.	1.3	80
58	Renal clearable Hafnium-doped carbon dots for CT/Fluorescence imaging of orthotopic liver cancer. Biomaterials, 2020, 255, 120110.	5.7	79
59	Activity of Specific Lipid-regulated ADP Ribosylation Factor-GTPase–activating Proteins Is Required for Sec14p-dependent Golgi Secretory Function in Yeast. Molecular Biology of the Cell, 2002, 13, 2193-2206.	0.9	78
60	Integration of metal-organic framework with a photoactive porous-organic polymer for interface enhanced phototherapy. Biomaterials, 2020, 235, 119792.	5.7	78
61	The use of polymeric platinum(IV) prodrugs to deliver multinuclear platinum(II) drugs with reduced systemic toxicity and enhanced antitumor efficacy. Biomaterials, 2012, 33, 8657-8669.	5.7	77
62	Zirconium-Based Nanoscale Metal–Organic Framework/Poly(ε-caprolactone) Mixed-Matrix Membranes as Effective Antimicrobials. ACS Applied Materials & Interfaces, 2017, 9, 41512-41520.	4.0	77
63	Lysosome targeting carbon dots-based fluorescent probe for monitoring pH changes in vitro and in vivo. Chemical Engineering Journal, 2020, 381, 122665.	6.6	77
64	A high connectivity metal–organic framework with exceptional hydrogen and methane uptake capacities. Chemical Science, 2012, 3, 3032.	3.7	75
65	Synthesis of mesoporous silica nanoparticle–oxaliplatin conjugates for improved anticancer drug delivery. Colloids and Surfaces B: Biointerfaces, 2014, 117, 75-81.	2.5	75
66	BODIPY-containing nanoscale metal–organic frameworks as contrast agents for computed tomography. Journal of Materials Chemistry B, 2017, 5, 2330-2336.	2.9	75
67	Biodegradable Amphiphilic Block Copolymers Bearing Protected Hydroxyl Groups: Synthesis and Characterization. Biomacromolecules, 2008, 9, 553-560.	2.6	73
68	BODIPY photocatalyzed oxidation of thioanisole under visible light. Catalysis Communications, 2011, 16, 94-97.	1.6	73
69	Light-Harvesting Cross-Linked Polymers for Efficient Heterogeneous Photocatalysis. ACS Applied Materials & Interfaces, 2012, 4, 2288-2294.	4.0	72
70	Transferrin-Conjugated Micelles: Enhanced Accumulation and Antitumor Effect for Transferrin-Receptor-Overexpressing Cancer Models. Molecular Pharmaceutics, 2012, 9, 1919-1931.	2.3	72
71	Activity of Specific Lipid-regulated ADP Ribosylation Factor-GTPase-activating Proteins Is Required for Sec14p-dependent Colgi Secretory Function in Yeast. Molecular Biology of the Cell, 2002, 13, 2193-2206.	0.9	72
72	Reduction-sensitive core-cross-linked mPEG–poly(ester-carbonate) micelles for glutathione-triggered intracellular drug release. Polymer Chemistry, 2012, 3, 2403.	1.9	71

#	Article	IF	CITATIONS
73	Biodegradable Amphiphilic Copolymer Containing Nucleobase: Synthesis, Self-Assembly in Aqueous Solutions, and Potential Use in Controlled Drug Delivery. Biomacromolecules, 2012, 13, 3004-3012.	2.6	70
74	Near-Infrared Emitting Fluorescent BODIPY Nanovesicles for in Vivo Molecular Imaging and Drug Delivery. ACS Applied Materials & Interfaces, 2014, 6, 16166-16173.	4.0	70
75	Sugars-grafted aliphatic biodegradable poly(L-lactide-co-carbonate)s by click reaction and their specific interaction with lectin molecules. Journal of Polymer Science Part A, 2007, 45, 3204-3217.	2.5	69
76	Electrochemical Water Oxidation with Carbon-Grafted Iridium Complexes. ACS Applied Materials & Interfaces, 2012, 4, 608-613.	4.0	69
77	Oneâ€step Preparation of Macroporous Polymer Particles with Multiple Interconnected Chambers: A Candidate for Trapping Biomacromolecules. Angewandte Chemie - International Edition, 2013, 52, 10625-10629.	7.2	69
78	Ugi Reaction of Natural Amino Acids: A General Route toward Facile Synthesis of Polypeptoids for Bioapplications. ACS Macro Letters, 2016, 5, 1049-1054.	2.3	69
79	Nanoscale Covalent Organic Frameworks with Donor–Acceptor Structure for Enhanced Photothermal Ablation of Tumors. ACS Nano, 2021, 15, 7638-7648.	7.3	69
80	Chiral carbon dots-based nanosensors for Sn(II) detection and lysine enantiomers recognition. Sensors and Actuators B: Chemical, 2020, 319, 128265.	4.0	69
81	Enhanced efficacy of photothermal therapy by combining a semiconducting polymer with an inhibitor of a heat shock protein. Materials Chemistry Frontiers, 2019, 3, 127-136.	3.2	68
82	Mitochondria-Targeting Organic Nanoparticles for Enhanced Photodynamic/Photothermal Therapy. ACS Applied Materials & Interfaces, 2020, 12, 30077-30084.	4.0	66
83	Porous heterogeneous organic photocatalyst prepared by HIPE polymerization for oxidation of sulfides under visible light. Journal of Materials Chemistry, 2012, 22, 17445.	6.7	64
84	Tetraphenylethylene-based fluorescent coordination polymers for drug delivery. Journal of Materials Chemistry B, 2016, 4, 4263-4266.	2.9	64
85	Time-programmed DCA and oxaliplatin release by multilayered nanofiber mats in prevention of local cancer recurrence following surgery. Journal of Controlled Release, 2016, 235, 125-133.	4.8	63
86	Photochromic Terbium Phosphonates with Photomodulated Luminescence and Metal Ion Sensitive Detection. Chemistry - A European Journal, 2016, 22, 15451-15457.	1.7	63
87	Ultrafast and Noninvasive Long-Term Bioimaging with Highly Stable Red Aggregation-Induced Emission Nanoparticles. Analytical Chemistry, 2019, 91, 3467-3474.	3.2	62
88	Evidence for an Intrinsic Toxicity of Phosphatidylcholine to Sec14p-dependent Protein Transport from the Yeast Golgi Complex. Molecular Biology of the Cell, 2001, 12, 1117-1129.	0.9	60
89	Photo-cross-linked mPEG-poly(γ-cinnamyl-l-glutamate) micelles as stable drug carriers. Polymer Chemistry, 2012, 3, 1300.	1.9	60
90	Mechanism and Effect of Polar Styrenes on Scandium atalyzed Copolymerization with Ethylene. Angewandte Chemie - International Edition, 2018, 57, 14896-14901.	7.2	60

#	Article	IF	CITATIONS
91	Use of asymmetric multilayer polylactide nanofiber mats in controlled release of drugs and prevention of liver cancer recurrence after surgery in mice. Nanomedicine: Nanotechnology, Biology, and Medicine, 2015, 11, 1047-1056.	1.7	59
92	Supramolecular Hybrids of AlEgen with Carbon Dots for Noninvasive Long-Term Bioimaging. Chemistry of Materials, 2016, 28, 8825-8833.	3.2	59
93	Supramolecular hybrids of carbon dots with doxorubicin: synthesis, stability and cellular trafficking. Materials Chemistry Frontiers, 2017, 1, 354-360.	3.2	59
94	Benzimidazole-BODIPY as optical and fluorometric pH sensor. Dyes and Pigments, 2016, 128, 165-169.	2.0	58
95	Carbon dots with concentration-modulated fluorescence: Aggregation-induced multicolor emission. Journal of Colloid and Interface Science, 2020, 573, 241-249.	5.0	58
96	Synthesis and characterization of amphiphilic block copolymers with allyl sideâ€groups. Journal of Polymer Science Part A, 2007, 45, 5518-5528.	2.5	57
97	Synthesis and Characterization of Novel Biodegradable Poly(carbonate ester)s with Photolabile Protecting Groups. Biomacromolecules, 2008, 9, 376-380.	2.6	57
98	Reduction-responsive shell-crosslinked micelles prepared from Y-shaped amphiphilic block copolymers as a drug carrier. Soft Matter, 2012, 8, 7426.	1.2	56
99	Near-Infrared Polymeric Nanoparticles with High Content of Cyanine for Bimodal Imaging and Photothermal Therapy. ACS Applied Materials & amp; Interfaces, 2016, 8, 24426-24432.	4.0	56
100	Mechanism and Effect of Polar Styrenes on Scandium atalyzed Copolymerization with Ethylene. Angewandte Chemie, 2018, 130, 15112-15117.	1.6	55
101	Ionic Covalentâ€Organic Framework Nanozyme as Effective Cascade Catalyst against Bacterial Wound Infection. Small, 2021, 17, e2100756.	5.2	55
102	Unadulterated BODIPY-dimer nanoparticles with high stability and good biocompatibility for cellular imaging. Nanoscale, 2014, 6, 5662-5665.	2.8	54
103	Selfâ€Assembly of Porphyrin–Paclitaxel Conjugates Into Nanomedicines: Enhanced Cytotoxicity due to Endosomal Escape. Chemistry - an Asian Journal, 2016, 11, 1780-1784.	1.7	54
104	Rational design of iridium–porphyrin conjugates for novel synergistic photodynamic and photothermal therapy anticancer agents. Chemical Science, 2021, 12, 5918-5925.	3.7	53
105	Targeting and anti-tumor effect of folic acid-labeled polymer–Doxorubicin conjugates with pH-sensitive hydrazone linker. Journal of Materials Chemistry, 2012, 22, 13303.	6.7	51
106	Injectable and biodegradable supramolecular hydrogels formed by nucleobase-terminated poly(ethylene oxide)s and α-cyclodextrin. Journal of Materials Chemistry B, 2014, 2, 659-667.	2.9	51
107	Two tetraphenylethene-containing coordination polymers for reversible mechanochromism. Chemical Communications, 2017, 53, 7048-7051.	2.2	51
108	Comparing Effects of Redox Sensitivity of Organic Nanoparticles to Photodynamic Activity. Chemistry of Materials, 2017, 29, 1856-1863.	3.2	50

#	Article	IF	CITATIONS
109	Core-crosslinked amphiphilic biodegradable copolymer based on the complementary multiple hydrogen bonds of nucleobases: synthesis, self-assembly and in vitro drug delivery. Journal of Materials Chemistry, 2012, 22, 24832.	6.7	49
110	Polymer brushes on metal–organic frameworks by UV-induced photopolymerization. Polymer Chemistry, 2016, 7, 5828-5834.	1.9	49
111	Nanoscale Fluorescent Metal–Organic Framework@Microporous Organic Polymer Composites for Enhanced Intracellular Uptake and Bioimaging. Chemistry - A European Journal, 2017, 23, 1379-1385.	1.7	49
112	Nanoscale Melittin@Zeolitic Imidazolate Frameworks for Enhanced Anticancer Activity and Mechanism Analysis. ACS Applied Materials & Interfaces, 2018, 10, 22974-22984.	4.0	49
113	Preparation of block copolymer of É›-caprolactone and 2-methyl-2-carboxyl-propylene carbonate. Polymer, 2005, 46, 2817-2824.	1.8	48
114	Solidâ€State TICTâ€Emissive Cruciform: Aggregationâ€Enhanced Emission, Deepâ€Red to Nearâ€Infrared Piezochromism and Imaging In Vivo. Advanced Optical Materials, 2018, 6, 1800956.	3.6	48
115	Inhibition of CD44 expression in hepatocellular carcinoma cells enhances apoptosis, chemosensitivity, and reduces tumorigenesis and invasion. Cancer Chemotherapy and Pharmacology, 2008, 62, 949-957.	1.1	47
116	Aliphatic poly(esterâ€carbonate)s bearing amino groups and its RGD peptide grafting. Journal of Polymer Science Part A, 2008, 46, 7022-7032.	2.5	47
117	Dynamically controlled one-pot synthesis of heterogeneous core–shell MOF single crystals using guest molecules. Chemical Communications, 2014, 50, 11653-11656.	2.2	47
118	Hybrid polymer micelles capable of cRGD targeting and pH-triggered surface charge conversion for tumor selective accumulation and promoted uptake. Chemical Communications, 2014, 50, 9188-9191.	2.2	46
119	BODIPY@carbon dot nanocomposites for enhanced photodynamic activity. Materials Chemistry Frontiers, 2019, 3, 1747-1753.	3.2	45
120	Fluorine-Doped Carbon Dots with Intrinsic Nucleus-Targeting Ability for Drug and Dye Delivery. Bioconjugate Chemistry, 2020, 31, 646-655.	1.8	45
121	The impact of the postharvest environment on the viability and virulence of decay fungi. Critical Reviews in Food Science and Nutrition, 2018, 58, 1681-1687.	5.4	44
122	Amphiphilic Polycarbonates from Carborane-Installed Cyclic Carbonates as Potential Agents for Boron Neutron Capture Therapy. Bioconjugate Chemistry, 2016, 27, 2214-2223.	1.8	43
123	Solvatochromic fluorescent carbon dots as optic noses for sensing volatile organic compounds. RSC Advances, 2016, 6, 83501-83504.	1.7	43
124	Engineering pH-Responsive BODIPY Nanoparticles for Tumor Selective Multimodal Imaging and Phototherapy. ACS Applied Materials & Interfaces, 2019, 11, 43928-43935.	4.0	43
125	Size-dependent biodistribution and antitumor efficacy of polymer micelle drug delivery systems. Journal of Materials Chemistry B, 2013, 1, 4273.	2.9	42
126	Single-Stimulus Dual-Drug Sensitive Nanoplatform for Enhanced Photoactivated Therapy. Biomacromolecules, 2016, 17, 2120-2127.	2.6	42

#	Article	IF	CITATIONS
127	Metal–Organic Frameworks@Polymer Composites Containing Cyanines for Near-Infrared Fluorescence Imaging and Photothermal Tumor Therapy. Bioconjugate Chemistry, 2017, 28, 2784-2793.	1.8	42
128	Metal–Organic Frameworks for Photodynamic Therapy: Emerging Synergistic Cancer Therapy. Biotechnology Journal, 2021, 16, e1900382.	1.8	42
129	pH-responsive metallo-supramolecular nanogel for synergistic chemo-photodynamic therapy. Acta Biomaterialia, 2015, 25, 162-171.	4.1	41
130	Small molecular nanomedicines made from a camptothecin dimer containing a disulfide bond. RSC Advances, 2015, 5, 81499-81501.	1.7	40
131	Cyanine-Curcumin Assembling Nanoparticles for Near-Infrared Imaging and Photothermal Therapy. ACS Biomaterials Science and Engineering, 2016, 2, 1942-1950.	2.6	40
132	Near infrared BODIPY-Platinum conjugates for imaging, photodynamic therapy and chemotherapy. Dyes and Pigments, 2017, 141, 5-12.	2.0	40
133	Hybrid Nanomaterials of Conjugated Polymers and Albumin for Precise Photothermal Therapy. ACS Applied Materials & Interfaces, 2019, 11, 278-287.	4.0	40
134	Bright red aggregation-induced emission nanoparticles for multifunctional applications in cancer therapy. Chemical Science, 2020, 11, 2369-2374.	3.7	40
135	Synthesis and Characterization of Biodegradable Amphiphilic Triblock Copolymers Containingl-Glutamic Acid Units. Biomacromolecules, 2005, 6, 1954-1960.	2.6	39
136	Exploring the optimal ratio of d-glucose/l-aspartic acid for targeting carbon dots toward brain tumor cells. Materials Science and Engineering C, 2018, 85, 1-6.	3.8	39
137	ABT-869, a multi-targeted tyrosine kinase inhibitor, in combination with rapamycin is effective for subcutaneous hepatocellular carcinoma xenograft. Journal of Hepatology, 2008, 49, 985-997.	1.8	38
138	Reduction-responsive fluorescence off–on BODIPY–camptothecin conjugates for self-reporting drug release. Journal of Materials Chemistry B, 2016, 4, 2332-2337.	2.9	38
139	Stereochemically Dependent Synthesis of Two Cu(I) Cluster-Based Coordination Polymers with Thermochromic Luminescence. Inorganic Chemistry, 2017, 56, 13975-13981.	1.9	38
140	Albumin-bound paclitaxel dimeric prodrug nanoparticles with tumor redox heterogeneity-triggered drug release for synergistic photothermal/chemotherapy. Nano Research, 2019, 12, 877-887.	5.8	38
141	Triblock poly(lactic acid)-b-poly(ethylene glycol)-b-poly(lactic acid)/paclitaxel conjugates: Synthesis, micellization, and cytotoxicity. Journal of Applied Polymer Science, 2007, 105, 2271-2279.	1.3	37
142	Three-Dimensional Metalâ^'Organic Frameworks Based on Tetrahedral and Square-Planar Building Blocks: Hydrogen Sorption and Dye Uptake Studies. Inorganic Chemistry, 2010, 49, 9107-9109.	1.9	37
143	Overcoming tumor resistance to cisplatin through micelle-mediated combination chemotherapy. Biomaterials Science, 2015, 3, 182-191.	2.6	37
144	Lanthanide-Connecting and Lone-Electron-Pair Active Trigonal-Pyramidal-AsO3 Inducing Nanosized Poly(polyoxotungstate) Aggregates and Their Anticancer Activities. Scientific Reports, 2016, 6, 26406.	1.6	37

#	Article	IF	CITATIONS
145	Co-assembled hybrids of proteins and carbon dots for intracellular protein delivery. Journal of Materials Chemistry B, 2016, 4, 5659-5663.	2.9	37
146	Facile synthesis of a metal–organic framework nanocarrier for NIR imaging-guided photothermal therapy. Biomaterials Science, 2018, 6, 2918-2924.	2.6	37
147	Photothermal-Controlled Generation of Alkyl Radical from Organic Nanoparticles for Tumor Treatment. ACS Applied Materials & Interfaces, 2019, 11, 5782-5790.	4.0	37
148	Carbon dots-based fluorescence and UV–vis absorption dual-modal sensors for Ag+ and l-cysteine detection. Dyes and Pigments, 2021, 187, 109126.	2.0	37
149	Room temperature phosphorescent carbon dots for latent fingerprints detection and in vivo phosphorescence bioimaging. Sensors and Actuators B: Chemical, 2022, 351, 130976.	4.0	37
150	Synergistic antileukemia effect of genistein and chemotherapy in mouse xenograft model and potential mechanism through MAPK signaling. Experimental Hematology, 2007, 35, 75.e1-75.e11.	0.2	36
151	Multifunctional Pt(<scp>iv</scp>) pro-drug and its micellar platform: to kill two birds with one stone. Journal of Materials Chemistry B, 2013, 1, 762-772.	2.9	36
152	Reduction-sensitive amphiphilic copolymers made via multi-component Passerini reaction for drug delivery. Colloids and Surfaces B: Biointerfaces, 2015, 126, 217-223.	2.5	36
153	A dextran–platinum(<scp>iv</scp>) conjugate as a reduction-responsive carrier for triggered drug release. Journal of Materials Chemistry B, 2015, 3, 8203-8211.	2.9	36
154	Amphiphilic redox-sensitive NIR BODIPY nanoparticles for dual-mode imaging and photothermal therapy. Journal of Colloid and Interface Science, 2019, 536, 208-214.	5.0	36
155	A facile approach to biodegradable poly(ε-caprolactone)-poly(ethylene glycol)-based polyurethanes containing pendant amino groups. European Polymer Journal, 2007, 43, 2080-2087.	2.6	35
156	Synthesis and characterization of novel poly(ester carbonate)s based on pentaerythritol. Journal of Polymer Science Part A, 2007, 45, 1737-1745.	2.5	35
157	Cyclodextrin/Paclitaxel Dimer Assembling Vesicles: Reversible Morphology Transition and Cargo Delivery. ACS Applied Materials & Interfaces, 2017, 9, 26740-26748.	4.0	35
158	Self-destructive PEG–BODIPY nanomaterials for photodynamic and photothermal therapy. Journal of Materials Chemistry B, 2019, 7, 4655-4660.	2.9	35
159	Hyaluronic acid nanofiber mats loaded with antimicrobial peptide towards wound dressing applications. Materials Science and Engineering C, 2021, 128, 112319.	3.8	35
160	Biomimetic nano-NOS mediated local NO release for inhibiting cancer-associated platelet activation and disrupting tumor vascular barriers. Biomaterials, 2020, 255, 120141.	5.7	35
161	A pharmaceutical hydrogen-bonded covalent organic polymer for enrichment of volatile iodine. RSC Advances, 2017, 7, 54407-54415.	1.7	35
162	Local, combination chemotherapy in prevention of cervical cancer recurrence after surgery by using nanofibers co-loaded with cisplatin and curcumin. RSC Advances, 2015, 5, 106325-106332.	1.7	34

#	Article	IF	CITATIONS
163	Glutathione-responsive paclitaxel dimer nanovesicles with high drug content. Biomaterials Science, 2017, 5, 1517-1521.	2.6	34
164	Multiantigenic Nanoformulations Activate Anticancer Immunity Depending on Size. Advanced Functional Materials, 2019, 29, 1903391.	7.8	34
165	Protein-assisted synthesis of nanoscale covalent organic frameworks for phototherapy of cancer. Materials Chemistry Frontiers, 2020, 4, 2346-2356.	3.2	34
166	Chiral Carbon Dots-Enzyme Nanoreactors with Enhanced Catalytic Activity for Cancer Therapy. ACS Applied Materials & Interfaces, 2021, 13, 56456-56464.	4.0	34
167	Relief of oxidative stress and cardiomyocyte apoptosis by using curcumin nanoparticles. Colloids and Surfaces B: Biointerfaces, 2017, 153, 174-182.	2.5	33
168	Synergistic enhancement of immunological responses triggered by hyperthermia sensitive Pt NPs via NIR laser to inhibit cancer relapse and metastasis. Bioactive Materials, 2022, 7, 389-400.	8.6	33
169	Novel biodegradable poly(ethylene glycol)-block-poly(2-methyl-2-carboxyl-propylene carbonate) copolymers: Synthesis, characterization, and micellization. Polymer, 2005, 46, 10523-10530.	1.8	32
170	Functional Metal–Organic Frameworks via Ligand Doping: Influences of Ligand Charge and Steric Demand. Inorganic Chemistry, 2014, 53, 1331-1338.	1.9	32
171	Acetalated-dextran as valves of mesoporous silica particles for pH responsive intracellular drug delivery. RSC Advances, 2015, 5, 9546-9555.	1.7	32
172	Nanoscale Metal–Organic Framework–Hemoglobin Conjugates. Chemistry - an Asian Journal, 2016, 11, 750-756.	1.7	32
173	PEGâ€Induced Synthesis of Coordinationâ€Polymer Isomers with Tunable Architectures and Iodine Capture. Chemistry - an Asian Journal, 2017, 12, 615-620.	1.7	32
174	PEGylated BODIPY assembling fluorescent nanoparticles for photodynamic therapy. Chinese Chemical Letters, 2017, 28, 1875-1877.	4.8	32
175	Tailoring the morphology of AlEgen fluorescent nanoparticles for optimal cellular uptake and imaging efficacy. Chemical Science, 2018, 9, 2620-2627.	3.7	32
176	Comparative study of two near-infrared coumarin–BODIPY dyes for bioimaging and photothermal therapy of cancer. Journal of Materials Chemistry B, 2019, 7, 4717-4724.	2.9	32
177	A new format of bispecific antibody: highly efficient heterodimerization, expression and tumor cell lysis. Journal of Immunological Methods, 2005, 296, 95-101.	0.6	31
178	Biological Characterization of Folate-Decorated Biodegradable Polymer–Platinum(II) Complex Micelles. Molecular Pharmaceutics, 2012, 9, 3200-3208.	2.3	31
179	Double pH-responsive supramolecular copolymer micelles based on the complementary multiple hydrogen bonds of nucleobases and acetalated dextran for drug delivery. Polymer Chemistry, 2015, 6, 3625-3633.	1.9	31
180	Hybrids of carbon dots with subunit B of ricin toxin for enhanced immunomodulatory activity. Journal of Colloid and Interface Science, 2018, 523, 226-233.	5.0	31

#	Article	IF	CITATIONS
181	Fused Isoindigo Ribbons with Absorption Bands Reaching Nearâ€Infrared. Angewandte Chemie - International Edition, 2018, 57, 10283-10287.	7.2	31
182	Defect Engineering of Nanoscale Hf-Based Metal–Organic Frameworks for Highly Efficient Iodine Capture. Inorganic Chemistry, 2021, 60, 9848-9856.	1.9	31
183	Phosphatidylinositol transfer protein function in the yeast Saccharomyces cerevisiae. Advances in Enzyme Regulation, 2005, 45, 155-170.	2.9	30
184	A Nanosized {Ag@Ag ₁₂ } "Molecular Windmill―Templated by Polyoxometalates Anions. Inorganic Chemistry, 2014, 53, 11584-11588.	1.9	30
185	A glutathione-activatable photodynamic and fluorescent imaging monochromatic photosensitizer. Journal of Materials Chemistry B, 2017, 5, 4239-4245.	2.9	30
186	Determinants of Sensitivity to DZNep Induced Apoptosis in Multiple Myeloma Cells. PLoS ONE, 2011, 6, e21583.	1.1	29
187	Synthesis of a Nearâ€Infrared BODIPY Dye for Bioimaging and Photothermal Therapy. Chemistry - an Asian Journal, 2018, 13, 989-995.	1.7	29
188	A convenient and universal platform for sensing environmental nitro-aromatic explosives based on amphiphilic carbon dots. Environmental Research, 2019, 177, 108621.	3.7	29
189	Leveraging BODIPY nanomaterials for enhanced tumor photothermal therapy. Journal of Materials Chemistry B, 2021, 9, 7318-7327.	2.9	29
190	Synthesis and self-assembly of a novel Y-shaped copolymer with a helical polypeptide arm. Polymer, 2009, 50, 455-461.	1.8	28
191	Near-Infrared-Light-Induced Morphology Transition of Poly(ether amine) Nanoparticles for Supersensitive Drug Release. ACS Applied Materials & Interfaces, 2018, 10, 7413-7421.	4.0	28
192	Rational Design of BODIPY-Diketopyrrolopyrrole Conjugated Polymers for Photothermal Tumor Ablation. ACS Applied Materials & Interfaces, 2019, 11, 32720-32728.	4.0	28
193	Rational design of BODIPY organic nanoparticles for enhanced photodynamic/photothermal therapy. Dyes and Pigments, 2019, 162, 295-302.	2.0	28
194	Comparison of Redox Responsiveness and Antitumor Capability of Paclitaxel Dimeric Nanoparticles with Different Linkers. Chemistry of Materials, 2020, 32, 10719-10727.	3.2	28
195	Indocyanine green potentiated paclitaxel nanoprodrugs for imaging and chemotherapy. Exploration, 2022, 2, .	5.4	28
196	Biodegradable Amphiphilic Triblock Copolymer Bearing Pendant Glucose Residues:Â Preparation and Specific Interaction with Concanavalin A Molecules. Biomacromolecules, 2006, 7, 1806-1810.	2.6	27
197	Cooperation of Amphiphilicity and Crystallization for Regulating the Self-Assembly of Poly(ethylene) Tj ETQq1 1	0.784314 1.6	rgBT /Overloo
198	Porphyrin–ferrocene conjugates for photodynamic and chemodynamic therapy. Organic and Biomolecular Chemistry, 2018, 16, 8613-8619.	1.5	27

#	Article	IF	CITATIONS
199	Exposure of Candida oleophila to sublethal salt stress induces an antioxidant response and improves biocontrol efficacy. Biological Control, 2018, 127, 109-115.	1.4	27
200	BODIPY Fluorescent Chemosensor for Cu2+ Detection and Its Applications in Living Cells: Fast Response and High Sensitivity. Journal of Fluorescence, 2014, 24, 841-846.	1.3	26
201	Selfâ€Assembly of Tunable Heterometallic Ln–Ru Coordination Polymers with Nearâ€Infrared Luminescence and Magnetocaloric Effect. Chemistry - A European Journal, 2017, 23, 2852-2857.	1.7	26
202	Near-infrared nanoparticles based on aza-BDP for photodynamic and photothermal therapy. Dyes and Pigments, 2019, 160, 71-78.	2.0	26
203	Plasma Membrane Proteomics Identifies Biomarkers Associated with MMSET Overexpression in T(4;14) Multiple Myeloma. Oncotarget, 2013, 4, 1008-1018.	0.8	26
204	A biodegradable diblcok copolymer poly(ethylene) Tj ETQq0 0 0 rgBT /Overlock 10 Tf 50 547 Td (glycol)â€∢i>blo Docetaxel and RGD conjugation. Journal of Applied Polymer Science, 2008, 110, 2961-2970.	ckâ€p 1.3	oly(<scp>L25</scp>
205	Novel hydroxyl-containing reduction-responsive pseudo-poly(aminoacid) via click polymerization as an efficient drug carrier. Polymer Chemistry, 2014, 5, 4488.	1.9	25
206	Thiadiazole molecules and poly(ethylene glycol)-block-polylactide self-assembled nanoparticles as effective photothermal agents. Colloids and Surfaces B: Biointerfaces, 2015, 136, 201-206.	2.5	25
207	Exploiting aggregation induced emission and twisted intramolecular charge transfer in a BODIPY dye for selective sensing of fluoride in aqueous medium and living cells. Journal of Photochemistry and Photobiology A: Chemistry, 2018, 358, 274-283.	2.0	25
208	Self-assembled nanostructured photosensitizer with aggregation-induced emission for enhanced photodynamic anticancer therapy. Science China Materials, 2020, 63, 136-146.	3.5	25
209	Polymer-metal-organic framework hybrids for bioimaging and cancer therapy. Coordination Chemistry Reviews, 2022, 456, 214393.	9.5	25
210	Synthesis and characterization of novel biotinylated biodegradable poly(ethylene) Tj ETQq0 0 0 rgBT /Overlock 1	0 Tf 50 30 4.1	12 Td (glycol)-
211	A highly efficient "metalloligand―strategy for the synthesis of ternary Ln–Ru–W hybrids. Chemical Communications, 2013, 49, 7911.	2.2	24
212	A reduction-sensitive carrier system using mesoporous silica nanospheres with biodegradable polyester as caps. Physical Chemistry Chemical Physics, 2013, 15, 14210.	1.3	24
213	Paclitaxel prodrug nanoparticles combining chemical conjugation and physical entrapment for enhanced antitumor efficacy. RSC Advances, 2014, 4, 38405-38411.	1.7	24
214	Dual-Sensitive Charge-Conversional Polymeric Prodrug for Efficient Codelivery of Demethylcantharidin and Doxorubicin. Biomacromolecules, 2016, 17, 2650-2661.	2.6	24
215	Dopamine carbon nanodots as effective photothermal agents for cancer therapy. RSC Advances, 2016, 6, 54087-54091.	1.7	24
216	Redox responsive paclitaxel dimer for programmed drug release and selectively killing cancer cells. Journal of Colloid and Interface Science, 2020, 580, 785-793.	5.0	24

#	Article	IF	CITATIONS
217	Vaginal drug delivery approaches for localized management of cervical cancer. Advanced Drug Delivery Reviews, 2021, 174, 114-126.	6.6	24
218	Reductionâ€5ensitive Fluorinatedâ€Pt(IV) Universal Transfection Nanoplatform Facilitating CT45â€Targeted CRISPR/dCas9 Activation for Synergistic and Individualized Treatment of Ovarian Cancer. Small, 2021, 17, e2102494.	5.2	24
219	Regulation of Conjugated Hemoglobin on Micelles through Copolymer Chain Sequences and the Protein's Isoelectric Aggregation. Macromolecular Bioscience, 2013, 13, 893-902.	2.1	23
220	A trivalent anti-erbB2/anti-CD16 bispecific antibody retargeting NK cells against human breast cancer cells. Biochemical and Biophysical Research Communications, 2003, 311, 307-312.	1.0	22
221	In vivo activity of ABT-869, a multi-target kinase inhibitor, against acute myeloid leukemia with wild-type FLT3 receptor. Leukemia Research, 2008, 32, 1091-1100.	0.4	22
222	Near-infrared BODIPY-paclitaxel conjugates assembling organic nanoparticles for chemotherapy and bioimaging. Journal of Colloid and Interface Science, 2018, 514, 584-591.	5.0	22
223	Facile preparation of a tetraphenylethylene-doped metal–organic framework for white light-emitting diodes. Journal of Materials Chemistry C, 2018, 6, 11701-11706.	2.7	22
224	A postmodification strategy to modulate the photoluminescence of carbon dots from blue to green and red: synthesis and applications. Journal of Materials Chemistry B, 2019, 7, 3840-3845.	2.9	22
225	Small nanoparticles bring big prospect: The synthesis, modification, photoluminescence and sensing applications of carbon dots. Chinese Chemical Letters, 2022, 33, 1659-1672.	4.8	22
226	Synthesis, selfâ€assembly in water, and cytotoxicity of MPEGâ€ <i>block</i> â€PLLA/DX conjugates. Journal of Biomedical Materials Research - Part A, 2009, 88A, 238-245.	2.1	21
227	MMSET: Role and Therapeutic Opportunities in Multiple Myeloma. BioMed Research International, 2014, 2014, 1-5.	0.9	21
228	Green Photocatalysis with Oxygen Sensitive BODIPYs under Visible Light. Catalysis Letters, 2014, 144, 308-313.	1.4	21
229	Lactose targeting oxaliplatin prodrug loaded micelles for more effective chemotherapy of hepatocellular carcinoma. Journal of Materials Chemistry B, 2014, 2, 2097.	2.9	21
230	Red fluorescent pyrazoline-BODIPY nanoparticles for ultrafast and long-term bioimaging. Organic and Biomolecular Chemistry, 2020, 18, 707-714.	1.5	21
231	Heavy atom substituted near-infrared BODIPY nanoparticles for photodynamic therapy. Dyes and Pigments, 2020, 178, 108348.	2.0	21
232	Asymmetric copolymer vesicles to serve as a hemoglobin vector for ischemia therapy. Biomaterials Science, 2014, 2, 1254.	2.6	20
233	Preparation of highly luminescent and color tunable carbon nanodots under visible light excitation for in vitro and in vivo bio-imaging. Journal of Materials Research, 2015, 30, 3386-3393.	1.2	20
234	A polymer–(multifunctional single-drug) conjugate for combination therapy. Journal of Materials Chemistry B, 2015, 3, 4913-4921.	2.9	20

#	Article	IF	CITATIONS
235	Rational Design of Polymeric Nanoparticles with Tailorable Biomedical Functions for Cancer Therapy. ACS Applied Materials & Interfaces, 2017, 9, 29612-29622.	4.0	20
236	Engineering Paclitaxel Prodrug Nanoparticles via Redox-Activatable Linkage and Effective Carriers for Enhanced Chemotherapy. ACS Applied Materials & amp; Interfaces, 2021, 13, 46291-46302.	4.0	20
237	Near-Infrared absorbing J-Aggregates of boron dipyrromethene for high efficient photothermal therapy. Journal of Colloid and Interface Science, 2021, 599, 476-483.	5.0	20
238	Highly efficient near-infrared BODIPY phototherapeutic nanoparticles for cancer treatment. Journal of Materials Chemistry B, 2020, 8, 5305-5311.	2.9	20
239	Cyclic RGD targeting nanoparticles with pH sensitive polymer–drug conjugates for effective treatment of melanoma. RSC Advances, 2014, 4, 55187-55194.	1.7	19
240	Novel multi-sensitive pseudo-poly(amino acid) for effective intracellular drug delivery. RSC Advances, 2015, 5, 31972-31983.	1.7	19
241	BODIPY derivatives as light-induced free radical generators for hypoxic cancer treatment. Journal of Materials Chemistry B, 2019, 7, 3976-3981.	2.9	19
242	Photoactive Metal–Organic Framework@Porous Organic Polymer Nanocomposites with pHâ€Triggered Type I Photodynamic Therapy. Advanced Materials Interfaces, 2020, 7, 2000504.	1.9	19
243	4,4-Difluoro-4-bora-3a,4a-diaza-s-indacene (BDPI)-Triphenylphosphine Nanoparticles as a Photodynamic Antibacterial Agent. ACS Applied Nano Materials, 2022, 5, 1500-1507.	2.4	19
244	Facile Preparation of a Thienoisoindigo-Based Nanoscale Covalent Organic Framework with Robust Photothermal Activity for Cancer Therapy. ACS Applied Materials & Interfaces, 2022, 14, 19129-19138.	4.0	19
245	Luteinizing-hormone-releasing-hormone-containing biodegradable polymer micelles for enhanced intracellular drug delivery. Journal of Materials Chemistry B, 2013, 1, 293-301.	2.9	18
246	GSH-triggered size increase of porphyrin-containing nanosystems for enhanced retention and photodynamic activity. Journal of Materials Chemistry B, 2017, 5, 4470-4477.	2.9	18
247	Unadulterated Organic Nanoparticles with Small Sizes for Robust Tumor Imaging and Photothermal Treatment. Advanced Functional Materials, 2021, 31, 2103714.	7.8	18
248	Multifunctional BODIPY for effective inactivation of Gram-positive bacteria and promotion of wound healing. Biomaterials Science, 2021, 9, 7648-7654.	2.6	18
249	Deep Tumor Penetrating Gold Nanoâ€Adjuvant for NIRâ€Iâ€Triggered In Situ Tumor Vaccination. Small, 2022, 18, e2200993.	5.2	18
250	Nanoparticle mediated delivery of a GST inhibitor ethacrynic acid for sensitizing platinum based chemotherapy. RSC Advances, 2014, 4, 61124-61132.	1.7	17
251	Coâ€ <scp>D</scp> elivery of Oxaliplatin and Demethylcantharidin via a Polymer–Drug Conjugate. Macromolecular Bioscience, 2014, 14, 588-596.	2.1	17
252	Effect of Molecular Structure on Stability of Organic Nanoparticles Formed by Bodipy Dimers. Langmuir, 2016, 32, 9575-9581.	1.6	17

#	Article	IF	CITATIONS
253	The Effect of Molecular Structure on Cytotoxicity and Antitumor Activity of PEGylated Nanomedicines. Biomacromolecules, 2018, 19, 1625-1634.	2.6	17
254	Carrier-free core–shell nanodrugs for synergistic two-photon photodynamic therapy of cervical cancer. Journal of Colloid and Interface Science, 2019, 535, 84-91.	5.0	17
255	Exploiting radical-pair intersystem crossing for maximizing singlet oxygen quantum yields in pure organic fluorescent photosensitizers. Chemical Science, 2020, 11, 10921-10927.	3.7	17
256	Structural diversity of nanoscale zirconium porphyrin MOFs and their photoactivities and biological performances. Journal of Materials Chemistry B, 2021, 9, 7760-7770.	2.9	17
257	An activatable fluorescent prodrug of paclitaxel and BODIPY. Journal of Materials Chemistry B, 2021, 9, 2308-2313.	2.9	17
258	Fluorescent nanoparticles with ultralow chromophore loading for long-term tumor-targeted imaging. Acta Biomaterialia, 2020, 111, 398-405.	4.1	17
259	Two-dimensional metal-organic frameworks: from synthesis to bioapplications. Journal of Nanobiotechnology, 2022, 20, 207.	4.2	17
260	A Novel Biodegradable and Lightâ€Breakable Diblock Copolymer Micelle for Drug Delivery. Advanced Engineering Materials, 2009, 11, B7.	1.6	16
261	Polypyrrole coated PLGA core–shell nanoparticles for drug delivery and photothermal therapy. RSC Advances, 2016, 6, 84269-84275.	1.7	16
262	Rapid Self-Assembly of Block Copolymers for Flower-Like Particles with High Throughput. Langmuir, 2016, 32, 13517-13524.	1.6	16
263	Constructing reduction-sensitive PEGylated NIRF mesoporous silica nanoparticles <i>via</i> a one-pot Passerini reaction for photothermal/chemo-therapy. Chemical Communications, 2018, 54, 11921-11924.	2.2	16
264	Antigen-enabled facile preparation of MOF nanovaccine to activate the complement system for enhanced antigen-mediated immune response. Biomaterials Science, 2019, 7, 4022-4026.	2.6	16
265	Self-quenching synthesis of coordination polymer pre-drug nanoparticles for selective photodynamic therapy. Journal of Materials Chemistry B, 2019, 7, 7776-7782.	2.9	16
266	Redoxâ€responsive Fluorescent Nanoparticles Based on Diselenideâ€containing AIEgens for Cell Imaging and Selective Cancer Therapy. Chemistry - an Asian Journal, 2019, 14, 1745-1753.	1.7	16
267	Co-delivery of all-trans-retinoic-acid and cisplatin(iv) prodrug based on polymer–drug conjugates for enhanced efficacy and safety. Journal of Materials Chemistry, 2012, 22, 25453.	6.7	15
268	Synthesis of cross-linked polymers via multi-component Passerini reaction and their application as efficient photocatalysts. RSC Advances, 2014, 4, 25114-25117.	1.7	15
269	cRGD targeted and charge conversion-controlled release micelles for doxorubicin delivery. RSC Advances, 2015, 5, 22957-22964.	1.7	15
270	Selfâ€Assembly of Amphiphilic Drug–Dye Conjugates into Nanoparticles for Imaging and Chemotherapy. Chemistry - an Asian Journal, 2016, 11, 3174-3177.	1.7	15

#	Article	IF	CITATIONS
271	Amphiphilic Cyanine–Platinum Conjugates as Fluorescent Nanodrugs. Chemistry - an Asian Journal, 2016, 11, 221-225.	1.7	15
272	Size-Tunable and Crystalline BODIPY Nanorods for Bioimaging. ACS Biomaterials Science and Engineering, 2018, 4, 1969-1975.	2.6	15
273	Metalâ€Organic Sheets for Efficient Drug Delivery and Bioimaging. ChemMedChem, 2020, 15, 416-419.	1.6	15
274	Self-assembly of glutamic acid linked paclitaxel dimers into nanoparticles for chemotherapy. Bioorganic and Medicinal Chemistry Letters, 2017, 27, 2493-2496.	1.0	14
275	Nanoparticles based on glycyrrhetinic acid modified porphyrin for photodynamic therapy of cancer. Organic and Biomolecular Chemistry, 2018, 16, 1591-1597.	1.5	14
276	BODIPY-based carbon dots as fluorescent nanoprobes for sensing and imaging of extreme acidity. Analytical Methods, 2018, 10, 1863-1869.	1.3	14
277	Solvent controlled self-assembly of π-stacked/H-bonded supramolecular organic frameworks from a <i>C</i> ₃ -symmetric monomer for iodine adsorption. CrystEngComm, 2019, 21, 1742-1749.	1.3	14
278	A cationic BODIPY photosensitizer decorated with quaternary ammonium for high-efficiency photodynamic inhibition of bacterial growth. Journal of Materials Chemistry B, 2022, 10, 4967-4973.	2.9	14
279	Fluorescence‣abeled Immunomicelles: Preparation, in vivo Biodistribution, and Ability to Cross the Blood–Brain Barrier. Macromolecular Bioscience, 2012, 12, 1209-1219.	2.1	13
280	Insight into the fabrication of polymeric particle based oxygen carriers. International Journal of Pharmaceutics, 2014, 468, 75-82.	2.6	13
281	Protein-Resistant Biodegradable Amphiphilic Graft Copolymer Vesicles as Protein Carriers. Macromolecular Bioscience, 2015, 15, 1304-1313.	2.1	13
282	A pH-responsive poly(ether amine) micelle with hollow structure for controllable drug release. RSC Advances, 2016, 6, 91940-91948.	1.7	13
283	Nanoprodrug of retinoic acid-modified paclitaxel. Organic and Biomolecular Chemistry, 2017, 15, 9611-9615.	1.5	13
284	MMSET I acts as an oncoprotein and regulates GLO1 expression in t(4;14) multiple myeloma cells. Leukemia, 2019, 33, 739-748.	3.3	13
285	Near-infrared-emitting AIE multinuclear cationic Ir(<scp>iii</scp>) complex-assembled nanoparticles for photodynamic therapy. Dalton Transactions, 2020, 49, 15332-15338.	1.6	13
286	Intracellular Enzyme-Responsive Profluorophore and Prodrug Nanoparticles for Tumor-Specific Imaging and Precise Chemotherapy. ACS Applied Materials & Interfaces, 2021, 13, 59708-59719.	4.0	13
287	Polymeric dinulcear platinum(ii) complex micelles for enhanced antitumor activity. Journal of Materials Chemistry B, 2013, 1, 744.	2.9	12
288	Core Crossâ€Linked Micelleâ€Based Nanoreactors for Efficient Photocatalysis. Chemistry - an Asian Journal, 2013, 8, 2807-2812.	1.7	12

#	Article	IF	CITATIONS
289	Rational design and synthesis of covalent organic polymers with hollow structure and excellent antibacterial efficacy. RSC Advances, 2014, 4, 40269-40272.	1.7	12
290	Fluorescent Protein Nanovessels: A New Platform to Generate Bio–Abiotic Hybrid Materials for Bioimaging. Advanced Functional Materials, 2017, 27, 1702051.	7.8	12
291	Controlled Growth of Metalâ€Organic Frameworks on Polymer Brushes. Chemistry - A European Journal, 2017, 23, 13337-13341.	1.7	12
292	Stable supramolecular porphyrin@albumin nanoparticles for optimal photothermal activity. Materials Chemistry Frontiers, 2019, 3, 1892-1899.	3.2	12
293	Robust organic nanoparticles for noninvasive long-term fluorescence imaging. Journal of Materials Chemistry B, 2019, 7, 6879-6889.	2.9	12
294	Poly(ε-caprolactone) modified organic dyes nanoparticles for noninvasive long term fluorescence imaging. Colloids and Surfaces B: Biointerfaces, 2019, 173, 884-890.	2.5	12
295	Phenylboronic acid modified carbon dots for improved protein delivery. Chemical Engineering Science, 2021, 237, 116586.	1.9	12
296	In vitro and in vivo antitumor effect of a trivalent bispecific antibody targeting ErbB2 and CD16. Cancer Biology and Therapy, 2008, 7, 1744-1750.	1.5	11
297	Biodegradable dextran vesicles for effective haemoglobin encapsulation. Journal of Materials Chemistry B, 2015, 3, 5753-5759.	2.9	11
298	Synthesis of the Hemoglobinâ€Conjugated Polymer Micelles by Thiol Michael Addition Reactions. Macromolecular Bioscience, 2016, 16, 906-913.	2.1	11
299	Vaginal delivery of mucus-penetrating organic nanoparticles for photothermal therapy against cervical intraepithelial neoplasia in mice. Journal of Materials Chemistry B, 2019, 7, 4528-4537.	2.9	11
300	A fluorescent sensor for intracellular Zn ²⁺ based on cylindrical molecular brushes of poly(2-oxazoline) through ion-induced emission. Polymer Chemistry, 2020, 11, 6650-6657.	1.9	11
301	Structural optimization of organic fluorophores for highly efficient photothermal therapy. Materials Chemistry Frontiers, 2021, 5, 284-292.	3.2	11
302	Merocyanine-paclitaxel conjugates for photothermal induced chemotherapy. Journal of Materials Chemistry B, 2021, 9, 2334-2340.	2.9	11
303	Carbon dots embedded hydrogel spheres for sensing and removing rifampicin. Dyes and Pigments, 2022, 198, 110023.	2.0	11
304	Binary dimeric prodrug nanoparticles for self-boosted drug release and synergistic chemo-photodynamic therapy. Journal of Materials Chemistry B, 2022, 10, 880-886.	2.9	11
305	A redox-responsive dihydroartemisinin dimeric nanoprodrug for enhanced antitumor activity. Journal of Nanobiotechnology, 2021, 19, 441.	4.2	11
306	Catalytic Synthesis of Fatty Acid Methyl Esters from Extremely Low Quality Greases. JAOCS, Journal of the American Oil Chemists' Society, 2011, 88, 1417-1424.	0.8	10

#	Article	IF	CITATIONS
307	Light-induced synthesis of cross-linked polymers and their application in explosive detection. European Polymer Journal, 2015, 63, 149-155.	2.6	10
308	Multifunctional single-drug loaded nanoparticles for enhanced cancer treatment with low toxicity in vivo. RSC Advances, 2016, 6, 20366-20373.	1.7	10
309	Photothermally induced accumulation and retention of polymeric nanoparticles in tumors for long-term fluorescence imaging. Journal of Materials Chemistry B, 2017, 5, 2491-2499.	2.9	10
310	Triple-BODIPY organic nanoparticles with particular fluorescence emission. Dyes and Pigments, 2017, 147, 241-245.	2.0	10
311	Fused Isoindigo Ribbons with Absorption Bands Reaching Nearâ€Infrared. Angewandte Chemie, 2018, 130, 10440-10444.	1.6	10
312	Revealing membrane permeability of polymersomes through fluorescence enhancement. Colloids and Surfaces B: Biointerfaces, 2018, 161, 156-161.	2.5	10
313	A Paclitaxel Prodrug Activatable by Irradiation in a Hypoxic Microenvironment. Angewandte Chemie, 2020, 132, 23398-23405.	1.6	10
314	Dual-sensitive dual-prodrug nanoparticles with light-controlled endo/lysosomal escape for synergistic photoactivated chemotherapy. Biomaterials Science, 2021, 9, 7115-7123.	2.6	10
315	Near-Infrared Light-Boosted Photodynamic-Immunotherapy based on sulfonated Metal-Organic framework nanospindle. Chemical Engineering Journal, 2022, 437, 135370.	6.6	10
316	Thymine Modified Amphiphilic Biodegradable Copolymers for Photoâ€ <scp>C</scp> rossâ€ <scp>L</scp> inked Micelles as Stable Drug Carriers. Macromolecular Bioscience, 2013, 13, 1593-1600.	2.1	9
317	EGFPâ€Based Protein Nanoparticles with Cellâ€Penetrating Peptide for Efficient siRNA Delivery. Macromolecular Bioscience, 2015, 15, 1484-1489.	2.1	9
318	Photo-cross-linked poly(ether amine) micelles for controlled drug release. RSC Advances, 2015, 5, 105880-105888.	1.7	9
319	Synergistic effect and drugâ€resistance relief of paclitaxel and cisplatin caused by Coâ€delivery using polymeric micelles. Journal of Applied Polymer Science, 2015, 132, .	1.3	9
320	Phenylboronic Acidâ€Crossâ€Linked Nanoparticles with Improved Stability as Dual Acidâ€Responsive Drug Carriers. Macromolecular Bioscience, 2017, 17, 1600227.	2.1	9
321	A BODIPY biosensor to detect and drive self-assembly of diphenylalanine. Chemical Communications, 2019, 55, 8564-8566.	2.2	9
322	Water-soluble cyclometalated Ir(<scp>iii</scp>) complexes as carrier-free and pure nanoparticle photosensitizers for photodynamic therapy and cell imaging. Dalton Transactions, 2020, 49, 11493-11497.	1.6	9
323	Photothermal Therapy Combined with Light-Induced Generation of Alkyl Radicals for Enhanced Efficacy of Tumor Treatment. ACS Applied Polymer Materials, 2020, 2, 4188-4194.	2.0	9
324	Nanoscale porphyrin assemblies based on charge-transfer strategy with enhanced red-shifted absorption. Journal of Colloid and Interface Science, 2022, 627, 554-561.	5.0	9

#	Article	IF	CITATIONS
325	Ruthenium complex immobilized on mesoporous silica as recyclable heterogeneous catalyst for visible light photocatalysis. Chemical Research in Chinese Universities, 2014, 30, 310-314.	1.3	8
326	Transcriptome profiling reveals differential gene expression associated with changes in the morphology and stress tolerance of the biocontrol yeast, Pichia cecembensis. Biological Control, 2018, 120, 36-42.	1.4	8
327	The crystal structures, spectrometric, photodynamic properties and bioimaging of β-β linked Bodipy oligomers. Journal of Luminescence, 2019, 212, 306-314.	1.5	8
328	Nanoscale aggregates of porphyrins: red-shifted absorption, enhanced absorbance and phototherapeutic activity. Materials Chemistry Frontiers, 2021, 5, 8333-8340.	3.2	8
329	A nearâ€infrared probe for detecting and interposing amyloid beta oligomerization in early Alzheimer's disease. Alzheimer's and Dementia, 2023, 19, 456-466.	0.4	8
330	Cross-linked polymers based on 2,5-disubstituted tetrazoles for unsaturated hydrocarbon detection. RSC Advances, 2013, 3, 21302.	1.7	7
331	Complex of cisplatin with biocompatible poly(ethylene glycol) with pendant carboxyl groups for the effective treatment of liver cancer. Journal of Applied Polymer Science, 2014, 131, n/a-n/a.	1.3	7
332	Y-shaped block copolymer (methoxy-poly(ethylene glycol))2-b-poly(l-glutamic acid): preparation, self-assembly, and use as drug carriers. RSC Advances, 2014, 4, 41588-41596.	1.7	7
333	Comparing the Rod-Like and Spherical BODIPY Nanoparticles in Cellular Imaging. Frontiers in Chemistry, 2019, 7, 765.	1.8	7
334	Diketopyrrolopyrrole-based carbon dots for photodynamic therapy. Nanoscale, 2018, 10, 10991-10998.	2.8	7
335	Mimetic sea cucumber-shaped nanoscale metal-organic frameworks composite for enhanced photodynamic therapy. Dyes and Pigments, 2022, 197, 109920.	2.0	7
336	Fluorinated paclitaxel prodrugs for potentiated stability and chemotherapy. Journal of Materials Chemistry B, 2021, 9, 9971-9979.	2.9	7
337	The difference of binding epitopes on human CD16 (FcγRIII) interacted with hIgG1 and monoclonal antibody B88-9. Molecular Immunology, 2004, 41, 93-98.	1.0	6
338	Self-assembled organic nanorods for dual chemo-photodynamic therapies. RSC Advances, 2018, 8, 5493-5499.	1.7	6
339	Multivariate Strategy Preparation of Nanoscale Ru-Doped Metal–Organic Frameworks with Boosted Photoactivity for Bioimaging and Reactive Oxygen Species Generation. Inorganic Chemistry, 2022, 61, 4647-4654.	1.9	6
340	Biodegradable polymersomes from fourâ€arm PEGâ€bâ€PDLLA for encapsulating hemoglobin. Journal of Applied Polymer Science, 2014, 131, .	1.3	5
341	Effects of preparation parameters on the properties of the crosslinked pectin nanofiber mats. Carbohydrate Polymers, 2021, 269, 118314.	5.1	5
342	Water-Dispersible Porous Aromatic Frameworks with Quasi-Amino Acid Structures via N–H Insertion Reactions. ACS Nano, 2022, 16, 6197-6205.	7.3	5

#	Article	IF	CITATIONS
343	Exploring BODIPY derivatives as photosensitizers for antibacterial photodynamic therapy. Photodiagnosis and Photodynamic Therapy, 2022, 39, 102901.	1.3	5
344	Studies on the biological character of a new pH-sensitive doxorubicin prodrug with tumor targeting using a LC-MS/MS method. Analytical Methods, 2014, 6, 3159.	1.3	4
345	A single-step emulsion approach to prepare fluorescent nanoscale coordination polymers for bioimaging. RSC Advances, 2014, 4, 14803-14806.	1.7	4
346	Photoluminescence: Three Colors Emission from S,N Co-doped Graphene Quantum Dots for Visible Light H2Production and Bioimaging (Advanced Optical Materials 3/2015). Advanced Optical Materials, 2015, 3, 359-359.	3.6	4
347	Light-induced synthesis of triazine N-oxide-based cross-linked polymers for effective photocatalytic degradation of methyl orange. RSC Advances, 2017, 7, 9309-9315.	1.7	4
348	Ir(III) Complex Dimer Nanoparticles for Photodynamic Therapy. ACS Medicinal Chemistry Letters, 2021, 12, 1374-1379.	1.3	4
349	Controlled synthesis of spindle-shaped terrylenediimide nanoparticles for enhanced tumor accumulation and treatment. Chemical Engineering Journal, 2021, 419, 129552.	6.6	4
350	Multiantigenic Nanovaccines: Multiantigenic Nanoformulations Activate Anticancer Immunity Depending on Size (Adv. Funct. Mater. 49/2019). Advanced Functional Materials, 2019, 29, 1970336.	7.8	3
351	Conjugated Polymers and Polymer Dots for Cell Imaging. , 2020, , 155-180.		3
352	Therapeutic potential of antisense oligodeoxynucleotides in downregulating p53 oncogenic mutations in cancers. Biotechnology Letters, 2011, 33, 221-228.	1.1	2
353	A general carbon dot-based platform for intracellular delivery of proteins. Soft Matter, 2022, 18, 2776-2781.	1.2	2
354	Cyclometallic iridium-based nanorods for chemotherapy/photodynamic therapy. Materials Letters, 2020, 266, 127346.	1.3	1
355	Self-assembling organic nanoparticles for bioimaging and cargo delivery. Journal of Controlled Release, 2017, 259, e140-e141.	4.8	0
356	Green Fluorescent Protein Nanovessel Serves as a Nucleolus Targeting Material and Molecule Carrier in Living Cells. Advanced Biology, 2019, 3, e1900047.	3.0	0
357	Self-assembly of chiral foldamers with alternating hydrophilic and hydrophobic side chains into acid-sensitive and solvent-exchangeable vesicular particles. Soft Matter, 2021, 17, 10073-10079.	1.2	0